Engineering Fracture Mechanics Vol. 25, No. 4, pp. 451–462, 1986
Printed in Great Britain.

0013-7944/86 $3.00 + 0.00
Pergamon Journals Ltd.

COMPUTATION OF STRESS INTENSITY FACTORS FOR PLATE BENDING VIA A PATH-INDEPENDENT INTEGRAL

HORACIO A. SOSA† and JEFFREY W. EISCHEN‡
†Graduate Student, Division of Applied Mechanics, Durand Building, Stanford University, Stanford, CA 94305, U.S.A.
‡Assistant Professor, Department of Mechanical and Aerospace Engineering, North Carolina State University, Raleigh, NC 27695-7910, U.S.A.

Abstract—A simple and accurate method to determine stress intensity factors in cracked plates subjected to bending loads is proposed. A new vector J defined in terms of the sum of line and domain integrals is derived and expressed in terms of plate resultant quantities through the use of Reissner's transverse shear theory. Mindlin's plate theory is also treated within this framework. Of particular interest is the accomodation of the effect of a distributed pressure load. Relationships between J and the stress intensity factors are presented and employed for solving several example problems with the aid of finite element analysis. Detailed modeling of the crack tip region is completely avoided with this formulation. The stress intensity factor is computed for the case of a square plate containing a through crack and subjected to uniform transverse pressure loading. The geometric boundary conditions and Poisson's ratio were treated as parameters in this analysis.

1. INTRODUCTION

THE ANALYSIS of plate members containing through thickness flaws and subjected to bending loading has been a subject of controversy during the past decade. Because the problem is essentially three-dimensional very few configurations admit closed-form solutions due to inherent mathematical complexities. Consequently some simplifications are mandatory in order to render the problem tractable. Unlike the case of thin plates acted on by in-plane loads, where the use of two-dimensional elasticity theory provides an effective means of deriving stress intensity factor solutions, predictions of elastic fields for comparable structures subjected to bending loads is influenced by the specific plate theory by which the analysis is performed. A final word has not been established on this aspect, though it seems that a simplified theory which accounts for the effect of transverse shear strains and satisfies appropriate physical boundary conditions at the crack surface, approaches, at least in a qualitative manner, general three-dimensional behavior. Purely numerical techniques, such as the finite element method, are common tools for solving crack problems associated with finite bodies. However the results are sometimes not only costly, but uncertainty surrounds direct determination of stress intensity factors at the crack tip. The use of a conservation law and its related path-independent integral is shown in this paper to overcome this difficulty.

Analytical solutions for finite cracked plates are very limited. Keer and Sve[6] presented an analysis based on classical plate theory and integral equations. Very recently, Boduroglu and Erdogan[3] analyzed a finite edge-loaded finite-width plate while incorporating Reissner's[9] transverse shear theory. Finite element numerical analyses addressing plate problems generally fall into two categories: one involving hybrid or singularity element formulations, and others where path-independent integrals are employed. Ahmad and Loo[1] developed a singular element based on classical plate theory. This analysis appears flawed as Mode II stress intensity factors were predicted for loadings symmetric with respect to the crack line. Yagawa and Nishioka[14] employed a singular element where behavior of the in-plane displacements was based on transverse shear theory while out-of-plane displacements were governed by classical plate theory. Reasonable results were obtained despite the apparent conflict of physical theories. Chen and Chen[13] proposed another element based on a very complex singularity formulation into which classical plate theory was embedded. Ye and Gallagher[15] created yet another singularity element based on classical plate theory. Watanabe *et. al.*[12] employed a thick shell element together with a three-dimensonal J integral formulation. Their expression for J required both line and domain integral evaluations. Alwar and Nambissan[2] showed that the use of three-dimensional elasticity elements leads to

the conclusion that the stress intensity factor varies linearly through the thicknesss only for thin plates.

In the present paper, a simple and accurate method for determining stress intensity factors for cracked plates subjected to various bending loads is proposed. A new vector **J**, defined solely in terms of familiar plate resultant quantities is introduced. The formulation is consistent with Reissner's transverse theory, with Mindlin's theory as a special case. Unlike prior formulations, the new integral accomodates the effect of transverse pressure loadings. Finite element stress analysis is used in conjunction with **J** to predict stress intensity factors in finite cracked plates. Numerical results are compared with some very recent and complex analytical solutions, and agreement is excellent over a wide range of crack lengths and plate thicknesses. Several new results are presented for the important problem of a square plate containing a through crack (central and edge) and subjected to transverse pressure combined with various geometric boundary conditions. The key feature of this formulation is that detailed attention need not be paid to the crack tip region. The proposed approach appears to be the simplest available for accurately predicting stress intensity factors in cracked plates.

2. MATHEMATICAL FORMULATION

In this section a summary of Reissner's equations[9], which govern bending of linear elastic plates, is presented. Taking the x_1, x_2 plane of a three dimensional Cartesian basis to coincide with the mid-plane of the plate, the displacement components $u_i(x_j)$† can be expressed as

$$u_1 = x_3\psi_1(x_1, x_2),\ u_2 = x_3\psi_2(x_1, x_2),\ u_3 = w(x_1, x_2) \tag{1}$$

where w is the linearly weighted average, taken over the thickness, of the transverse displacement. Likewise, ψ_1 and ψ_2 are the linearly weighted averages of the rotation about the x_2 and x_1 axes, respectively, of fibers normal to the mid-plane prior to deformation. Collectively, w, ψ_1, ψ_2 are often referred to as *plate displacements*. Figure 1 depicts the sign conventions used throughout this paper. The following strain measures are introduced

$$\begin{aligned} &\Gamma_{11} = \frac{\partial\psi_1}{\partial x_1},\ \Gamma_{22} = \frac{\partial\psi_2}{\partial x_2} \\ &\Gamma_{12} = \frac{\partial\psi_2}{\partial x_1}+\frac{\partial\psi_1}{\partial x_2},\ \Gamma_{13} = \psi_1+\frac{\partial w}{\partial x_1},\ \Gamma_{23} = \psi_2+\frac{\partial w}{\partial x_2}. \end{aligned} \tag{2}$$

Bending and twisting moment resultant quantities are denoted by M_{11}, M_{22}, and M_{12}, respectively. Transverse shear force resultants are given by Q_1 and Q_2. The following constitutive relationship is appropriate, consistent with Reissner's theory

$$\begin{bmatrix} M_{11} \\ M_{22} \\ M_{12} \\ Q_1 \\ Q_2 \end{bmatrix} = D\begin{bmatrix} 1 & \nu & 0 & 0 & 0 \\ \nu & 1 & 0 & 0 & 0 \\ 0 & 0 & (1-\nu)/2 & 0 & 0 \\ 0 & 0 & 0 & C_s/D & 0 \\ 0 & 0 & 0 & 0 & C_s/D \end{bmatrix}\begin{bmatrix} \Gamma_{11} \\ \Gamma_{22} \\ \Gamma_{12} \\ \Gamma_{13} \\ \Gamma_{23} \end{bmatrix} + \hat{p}\begin{bmatrix} 1 \\ 1 \\ 0 \\ 0 \\ 0 \end{bmatrix} \tag{3}$$

where D, C_s, and $\hat{p}$ are given by

$$D = \frac{Eh^3}{12(1-\nu^2)},\ C_s = \frac{5}{6}Gh,\ \hat{p} = \frac{\nu h^2}{10(1-\nu)}p \tag{4}$$

and where E, G and ν are Young's modulus, the shear modulus and Poisson's ratio, respectively. The magnitude of the transverse pressure loading is denoted by $p = p(x_1, x_2)$. Mindlin[8] proposed

†The summation convention is implied when repeated indices appear. Latin and Greek subscripts have the range 1,2, and 1,2...5, respectively. An index preceeded by a comma indicates partial differentiation with respect to the associated index.

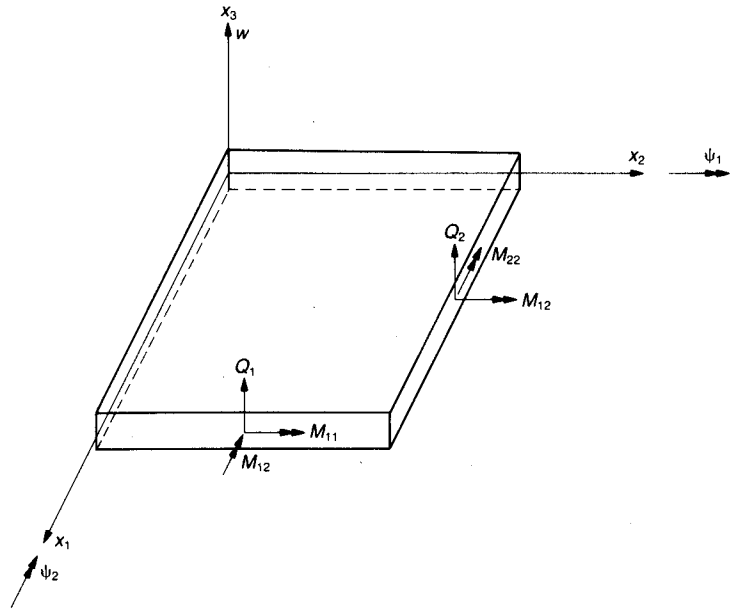

Fig. 1. Sign conventions for plate quantities.

a consonant constitutive relationship where the term in eq. (3) involving $\hat{p}$ is absent. Numerical results to be presented later in the paper explore the ramifications of ignoring such a term. Three column matrices are introduced in order to facilitate a more compact notation

$$\mathbf{f} = \begin{bmatrix} M_{11} \\ M_{22} \\ M_{12} \\ Q_1 \\ Q_2 \end{bmatrix}, \gamma = \begin{bmatrix} \Gamma_{11} \\ \Gamma_{22} \\ \Gamma_{12} \\ \Gamma_{13} \\ \Gamma_{23} \end{bmatrix}, \mathbf{p} = \hat{p} \begin{bmatrix} 1 \\ 1 \\ 0 \\ 0 \\ 0 \end{bmatrix}. \tag{5}$$

The constitutive relationship may then be written in the form

$$\mathbf{f} = \mathbf{C}\gamma + \hat{\mathbf{p}} \tag{6}$$

where $\mathbf{C}$ is a matrix whose entries should be clear upon examining eq. (3).

Moment and shear force resultant quantities satisfy the following equilibrium equations

$$\begin{aligned} \frac{\partial M_{11}}{\partial x_1} + \frac{\partial M_{12}}{\partial x_2} &= Q_1 \\ \frac{\partial M_{12}}{\partial x_1} + \frac{\partial M_{22}}{\partial x_2} &= Q_2 \\ \frac{\partial Q_1}{\partial x_1} + \frac{\partial Q_2}{\partial x_2} &= -p(x_1, x_2). \end{aligned} \tag{7}$$

An expression for the strain energy density W will be necessary during subsequent derivations. This quantity may be written as

$$W = \frac{1}{2}\left[\gamma^T \mathbf{C}\gamma - \frac{1}{D(1+\nu)}\mathbf{p}^T\mathbf{p}\right] \tag{8}$$

where the right superscript ^{T} indicates a matrix transpose operation. Furthermore, it can be shown that

$$\mathbf{f} = \frac{\partial W}{\partial \gamma} + \mathbf{p}. \tag{9}$$

These expressions are used in the sequel.

3. CONSERVATION LAW

A conservation law which proves useful for computing stress intensity factors in cracked plates can be derived in a direct manner by considering the gradient of W. The strain energy density function may be viewed as a function of the matrix γ and the matrix $\mathbf{p}$, i.e. $W = W(\gamma, \mathbf{p})$. Consequently

$$\frac{\partial W}{\partial x_k} = \frac{\partial W}{\partial \gamma_\alpha}\frac{\partial \gamma_\alpha}{\partial x_k} + \frac{\partial W}{\partial p_\alpha}\frac{\partial p_\alpha}{\partial x_k} \tag{10}$$

Substituting eq. (9) produces

$$W_{,k} - (f_\alpha - p_\alpha)\gamma_{\alpha,k} + \frac{1}{D(1+\nu)} p_\alpha p_{\alpha,k} = 0. \tag{11}$$

If the equilibrium equations are then introduced in eq. (11), it can be shown that

$$\begin{aligned} &W_{,k} - [(M_{11} - \hat{p})\psi_{1,k} + M_{12}\psi_{2,k} + Q_1 w_{,k}]_{,1} \\ &\quad - [M_{12}\psi_{1,k} + (M_{22} - \hat{p})\psi_{2,k} + Q_2 w_{,k}]_{,2} \\ &\quad - p w_{,k} - (\hat{p}_{,1}\psi_{1,k} + \hat{p}_{,2}\psi_{2,k}) + \frac{2}{D(1+\nu)}\hat{p}\hat{p}_{,k} = 0. \end{aligned} \tag{12}$$

Integrating eq. (12) over a domain Ω enclosed by the closed curve Γ and applying the divergence theorem yields

$$\begin{aligned} &\oint_\Gamma \{(W - pw)n_k - [(M_{11} - \hat{p})\psi_{1,k} + M_{12}\psi_{2,k} + Q_1 w_{,k}]n_1 - [(M_{22} - \hat{p})\psi_{2,k} + M_{12}\psi_{1,k} + Q_2 w_{,k}]n_2\}\, d\Gamma \\ &\quad + \int_\Omega [p_{,k} w - (\hat{p}_{,1}\psi_{1,k} + \hat{p}_{,2}\psi_{2,k}) + \frac{2}{D(1+\nu)}\hat{p}\,\hat{p}_{,k}]\, d\Omega = 0. \end{aligned} \tag{13}$$

If the applied pressure p is taken to be constant, such that $p_{,k} = 0$, the domain integral in eq. (13) vanishes. The integral expression given by the left hand side of eq. (13) can be defined as J_k, $k = 1,2$. The measure numbers J_k are equal to zero only if the region enclosed by the path Γ is free of defects. When the path Γ completely surrounds a defect embedded within a plate, such as a crack, J_k is path-domain independent and its magnitude provides the energy-release rate due to a translation of the entire defect in the k-direction. For the case when $k = 1$, J_1 is path-domain independent when an *open* path surrounds one tip of a sharp crack which lies along the x_1 axis. The J_2 integral does not possess this property in general.

The J_k integrals are particularly useful when related to the stress intensity factors for a crack problem. The general means of establishing this relationship is by substituting the near tip asymptotic behavior of the quantities into the integrand of eq. (13), and then integrating over a vanishingly small path (and associated domain) embracing the crack tip. The variation of the components of $\mathbf{f}$ is measured with respect to a cylindrical coordinate system (r, θ) fixed at the

crack tip. The angle θ is measured in a counterclockwise sense such that the upper and lower faces of the crack are located at $\theta = \pm\pi$, respectively. The use of eigenfunction series expansions [4] and Reissner's plate equations leads to the asymptotic behavior of the components of $\mathbf{f}$ and γ. It seems that the series expansions for the generalized displacement quantities have not been reported previously in the literature. These results (which will be presented in detail in another paper) are summarized in the Appendix. Observe that the stress intensity factors appear not only in the singular terms $[O(r^{-1/2})]$ of $\mathbf{f}$, but also in certain $O(r^{1/2})$ terms. An appropriate path for use in obtaining the relationship $J_1 = J_1(K_1, K_2, K_3)$ is a vanishingly small circular path centered at the crack tip. As $r \to 0$, only the singular terms $[O(r^{-1})]$ contribute to the final result

$$J_1 = \frac{12\pi}{Eh^3}\left[K_1^2 + K_2^2 + \frac{h^2}{10}(1+\nu)K_3^2 \right] \tag{14}$$

where the moment and shear force intensity factors are defined as follows

$$K_1 = \lim_{r\to 0} \sqrt{2r} M_{22}(r, 0),\ K_2 = \lim_{r\to 0} \sqrt{2r} M_{12}(r, 0),\ K_3 = \lim_{r\to 0} \sqrt{2r} Q_2(r, 0). \tag{15}$$

It should be recalled that within the transverse shear theory, bending stresses vary linearly through the plate thickness, while transverse shear stresses vary parabolically. This sometimes motivates the introduction of stress intensity factors which depend on the x_3 coordinate, and are related to K_1, K_2 and K_3 as follows

$$k_1(x_3) = \frac{12x_3}{h^3} K_1;\ k_2(x_3) = \frac{12x_3}{h^3} K_2;\ k_3(x_3) = \frac{3}{2h}\left[1 - \left(\frac{2x_3}{h}\right)^2 \right] K_3. \tag{16}$$

In order to obtain the relation between J_2 and the intensity factors, the same procedure is employed leading to

$$J_2^{\text{tip}} = -\frac{24\pi}{Eh^3} K_1 K_2. \tag{17}$$

The superscript on J_2 indicates explicitly that eq. (17) is valid only for a path such that $r \to 0$ since this integral is not path-independent when taken around one crack tip. If the J_2 integral is taken around a remote open path, it is found that

$$J_2 = -\frac{24\pi}{Eh^3} K_1 K_2 + \int_{\Gamma_c} [W - pw]\ \mathrm{d}x_1 \tag{18}$$

where the notation $[W-pw]$ indicates a discontinuity (or "jump") in the enclosed quantity across the crack surfaces. The symbol Γ_c denotes a path extending along the upper and lower crack surfaces. The use of eq. (18) together with J_1 and another path-independent integral for mixed modes will be the subject of a forthcoming paper.

4. FINITE ELEMENT IMPLEMENTATION

A wide choice of element types is available for analysis of plate bending problems. The goal of the present research has been to suggest a numerical technique for predicting stress intensity factors while avoiding complicated formulations, such as hybrid or singularity elements. The element selected was from the "Serendipity" quadrilateral family and possessed eight nodes, four corner and four midside. Three degrees of freedom were present at each node, rotations ψ_1 and ψ_2, together with the transverse displacement w. Uniform reduced integration was employed to avoid the "locking" phenomena associated with thin plate elements of this type. Two-by-two Gaussian

quadrature was employed to evaluate both the bending and transverse shear terms in the element stiffness matrices. A further description and accuracy assessment of this element is found in the book by Zienkiewicz[15]. While it is often claimed that the 9-node Lagrange element is superior to the 8-node Serendipity element, the authors proceeded with the latter element because of its availability in a pre-existing computer code. None of the problems typically plaguing the 8-node element (hourglassing) were encountered in the many numerical experiments conducted.

Because the inclusion of Reissner's constitutive equations does not appear to have been addressed before by finite element researchers, verification of the present formulation in the absence of a crack was appropriate. Enforcing the stationarity of the total potential energy, or equivalently developing an appropriate weak form of Reissner's plate equations, leads to the following variational statement

$$\int_A \delta^T \gamma \mathbf{C} \gamma \mathrm{d}A = \int_A p\delta w \mathrm{d}A + \int_{S_h} Q_i n_i \delta w \mathrm{d}S + \int_{S_h} M_{ij} n_j \delta \psi_i \mathrm{d}S - \int_A \hat{p}\delta\psi_{i,i}\mathrm{d}A + \int_A \hat{p}_{,i}\delta\psi_i \mathrm{d}A \tag{19}$$

where A is the area enclosed by the finite element mesh, and S_h is the portion of the boundary subjected to tractions. This equation should be of form familiar to numerical analysts. Reissner's constitutive equations are incorporated by appending domain integral terms to the right hand side of the finite element equations, much the same as in an initial stress problem. The stiffness matrix is identical for both the Mindlin and Reissner plate problems. To illustrate the effect of the constitutive equation on the lateral deflection w, a square plate (dimensions $2b \times 2b \times h$) subjected to uniform transverse pressure was analyzed. A 5×5 grid of square elements was used to model one quarter of the plate. Figure 2 shows the deflection of the center of the plate as a function of the thickness to length ratio $h/2b$. The deflection has been normalized with respect to the deflection predicted by classical plate theory ($w = 0.00406p(2b)^4/D$). Salerno and Goldberg[11] derived an exact solution for this problem using Reissner's equations. The present numerical results agree very closely with their predictions. The numerical results also agree with an earlier finite element analysis of this problem by Yagawa and Nishioka[14], who employed degenerated solid elements. They were surprised that their results agreed with Mindlin's theory rather than Reissner's. The reason for this is clear; their formulation did not account for the pressure dependent terms in the constitutive equation.

Figure 3 shows the finite element mesh, consisting of 140 elements and 469 nodes, employed to solve several crack boundary value problems. The boundary condition depicted in the figure is applicable for a central crack of length $2a$ in a square plate with dimensions $2b \times 2b$. Only loadings symmetric with respect to the x_1 axis were considered in this paper, and therefore only one quarter of the square plate required analysis. Crack length was varied simply by altering the

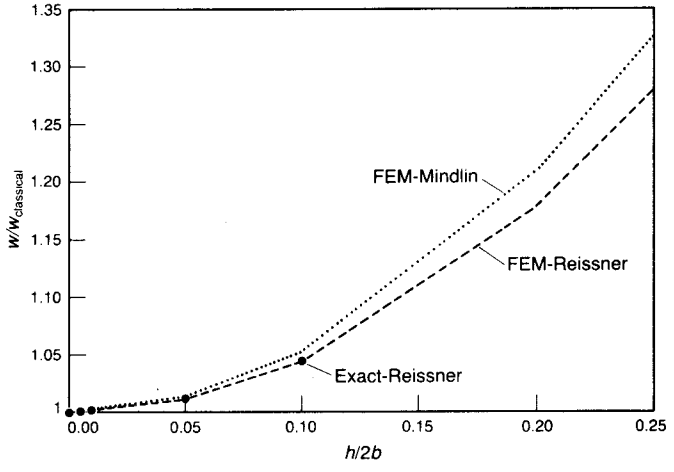

Fig. 2. Effect of plate thickness and constitutive relationship on the normalized transverse displacement.

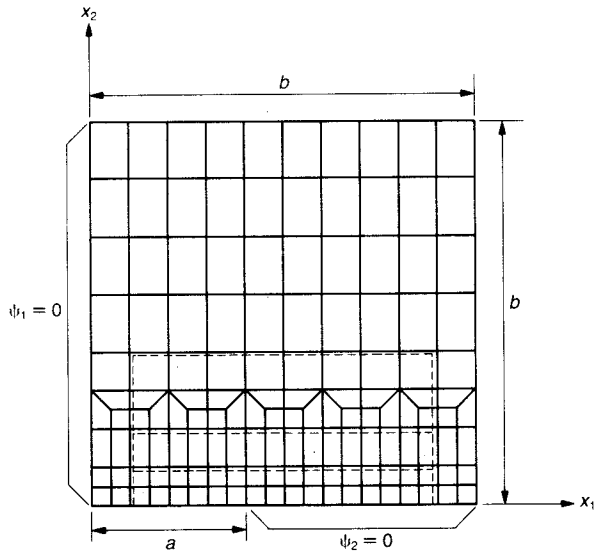

Fig. 3. Finite element mesh and J integral paths.

boundary condition on the edge $x_2 = 0$. This is a distinct advantage over formulations involving singularity elements where remeshing is required when the crack length is modified. Three integration paths were selected to evaluate the J_1 integral. It should be noted that for the problems under consideration in this paper, $K_2 = K_3 = 0$ and therefore $J_2 = 0$. Multiple domains were employed to verify the path-independence of the new J_1 integral, thereby providing a check on the numerical consistency of the results. The J_1 integral paths followed element edges, thus requiring evaluation of field quantities (M_{11}, Q_1, etc.) there. Field quantities were computed at the 2×2 Gauss integration points and then smoothed to the element edges according to the procedure advocated by Hinton[5].

5. NUMERICAL RESULTS

In order to verify the validity of the proposed approach, two problems concerning the bending of a square plate under the action of edge moments were studied. The results are compared with those of Boduroglu and Erdogan[3], which were produced by numerical solution of singular integral equations. Figure 4 shows the normalized moment intensity factor as a function of three length parameters (crack length a, plate dimensions b and h) for the case of a central crack of length $2a$. The following data were used for finite element analysis: $E = 1000$, $\nu = 0.3$, $b = 1$. The results are seen to agree very closely with those in ref. [3]. Three different paths were used in order to

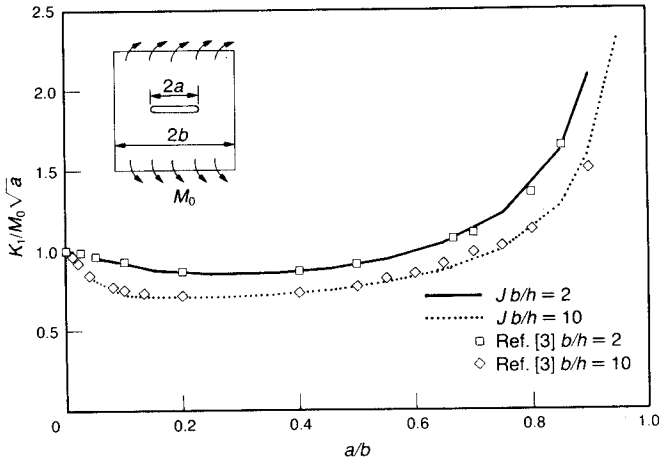

Fig. 4. Normalized moment intensity factor for a square plate containing a central crack and subjected to edge moment loading.

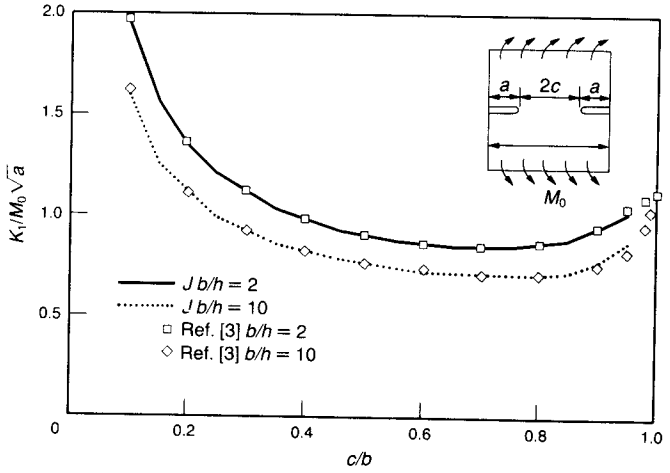

Fig. 5. Normalized moment intensity factor for a square plate containing edge cracks and subjected to edge moment loading.

verify path-independence. The difference between the extreme values was at most 2%. A very coarse mesh was constructed to ascertain the robustness of the new J_1 integral. The mesh consisted of 5×5 grid of square elements. It should be noted that for crack lengths in the range $0.3 \leqslant a \leqslant 0.6$, agreement within 6% was obtained between the coarse mesh and the mesh described in Fig. 3. In order to report accurate short and long crack results, a finer mesh (although still simple) was prepared. Results for this mesh are reported for crack lengths $a/b \leqslant 0.15$ and $a/b \geqslant 0.85$. The numerical results capture the very short crack behavior quite well, particularly for the thicker plate. The slight discrepancy between thin and thick plate results is due to the type of element used. If the classical plate theory was used, then the values of the normalized moment intensity factors would always be greater than one. Instead, the effect of shear deformation reduces the values in the short crack range. As the plate becomes vanishingly thin, the minimum value would approach $(1+\nu)/(3+\nu)$, as predicted by Knowles and Wang[7].

Figure 5 represents the normalized moment intensity factors for the same square plate containing two edge cracks. Note that the curves do not decrease monotonically for increasing c/b, rather at approximately $c/b = 0.7$, the moment intensity factor rises towards the limiting value 1.12 predicted by the in-plane theory and verified by ref. [3]. Boduroglu and Erdogan's[3] results are valid only for a plate unbounded in the x_2 direction. However, the numerical results proved that the plate dimension in the direction perpendicular to the crack line does not significantly affect the stress intensity factor.

Figures 6, 7 and 8 describe the effect of crack length, thickness, and boundary conditions on the moment intensity factor for the case of square plates subjected to uniform pressure. This mode

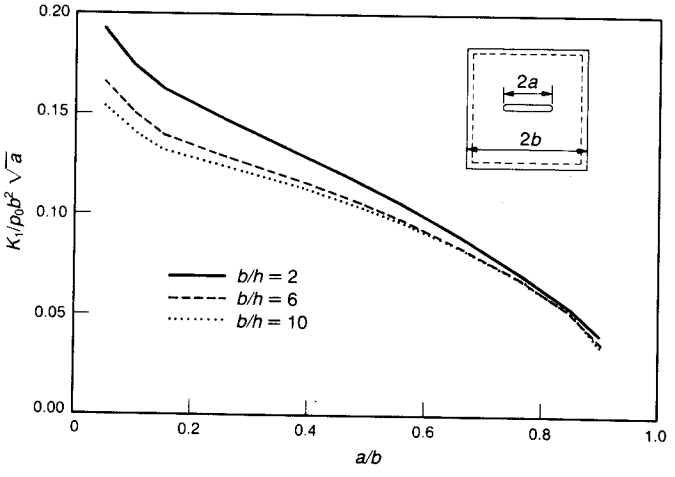

Fig. 6. Normalized moment intensity factor for a square plate containing a central crack and subjected to uniform pressure loading (simply supported all around).

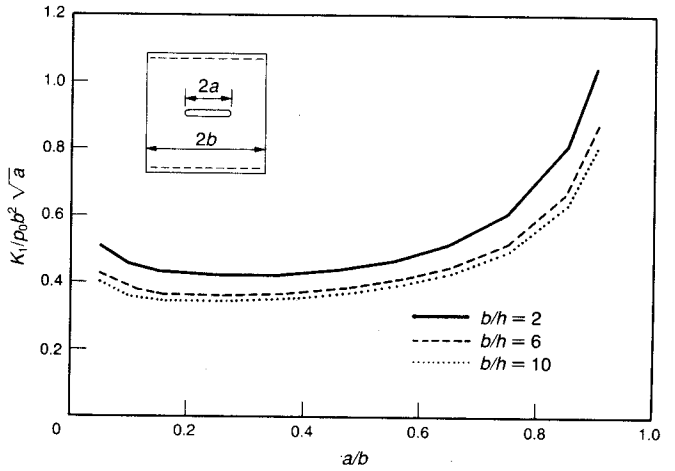

Fig. 7. Normalized moment intensity factor for a square plate containing a central crack and subjected to uniform pressure loading (simply supported on two edges).

of loading is important in aerospace structures. These results were all produced using Mindlin's constitutive equations. Figure 6 represents the case of all around simple supports with a central crack for three different thicknesses. It is very interesting to observe that the normalized moment intensity factor decreases with increasing crack length, due to the geometrically constrained boundary. In contrast, Fig. 7 shows the same plate and loading condition when the edges $x_1 = \pm b$ are free, resulting in rapid growth of K_1 when crack break-through occurs. Figure 8 presents results for the case of two edge cracks.

The effect of Poisson's ratio and the assumed constitutive relationships were also studied. Unlike plane elasticity fracture problems, the stress intensity factors for cracked plates depend on the magnitude of ν. Table 1 shows this dependence for the case of square plate with a central crack and having two edges simply supported. For the range of ν analyzed, the moment intensity factors are affected by at most 7%.

Table 1. Effect of Poisson's ratio on normalized moment intensity factor for a simply supported square plate with a central crack, $b/h = 10$

	$K_1/p_0b^2\sqrt{a}$		
a/b	$\nu = 0.1$	$\nu = 0.3$	$\nu = 0.45$
0.35	0.33957	0.35234	0.36196
0.55	0.37529	0.38965	0.40013
0.75	0.47672	0.49387	0.50593

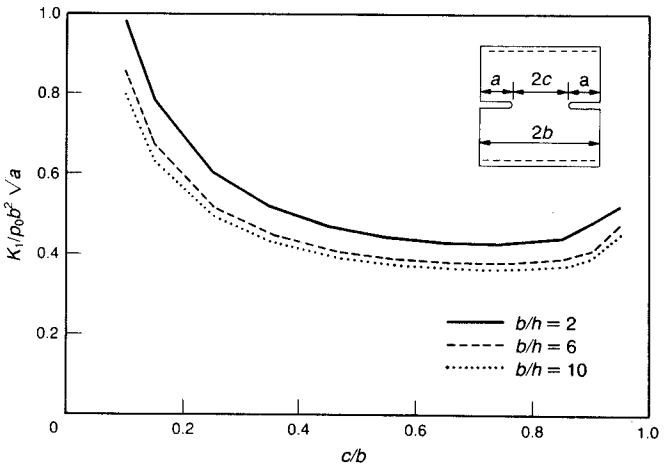

Fig. 8. Normalized moment intensity factor for a square plate containing two edge cracks and subjected to uniform pressure loading (simply supported on two edges).

Table 2. Normalized moment intensity factor computed via Mindlin's/Reissner's theory for a simply supported square plate with a central crack, $\nu = 0.3$

	$K_1/p_0b^2\sqrt{a}$	
a/b	$b/h = 10$	$b/h = 2$
0.35	0.35234/0.35214	0.42300/0.41707
0.55	0.38965/0.38946	0.46551/0.46004
0.75	0.49387/0.49370	0.60738/0.60249

Table 2 exemplifies the impact on the moment intensity factors of the difference between the Reissner's and Mindlin's constitutive relationships. It is surprising to note that the differences are almost insignificant when recalling the discrepancies between both theories in predicting the deflections of a perfect plate approached 4%. The present data shows instead that the energy release rate does not suffer a substantial change, despite the fact that the expression for J_1 is quite dependent on the plate theory employed. In all cases the moment intensity factors predicted by Mindlin's theory are higher than with Reissner's theory, which ignores the pressure dependent terms in the constitutive relationship, and is higher for shorter cracks and thicker plates.

6. CONCLUSIONS

The derivation of a conservation law in terms of plate resultant quantities, or equivalently a path-domain independent integral has been shown in a direct manner.

The use of a J_1 integral applicable to plates in conjunction with a finite element formulation has been applied to the bending of plates containing through thickness cracks. Unlike previous formulations, the effect of a distributed load is also accounted for.

The proposed method of solution has been illustrated by solving several problems. New results were provided for the case of a square plate loaded by a uniform pressure.

Acknowledgements—Financial support for this work from the DOE Grant 12040 and from AFOSR Grant 0149 to Stanford University is greatly appreciated. One of the authors (H. S.) wishes to thank Dr. Pawel Rafalski for useful comments on the subject.

REFERENCES

[1] J. Ahmad and F. T. Loo, Solution of plate bending problems in fracture mechanics using a specialized finite element technique. *Engng Fracture Mech.* **11,** 661–673 (1979).
[2] R. S. Alwar and K. N. R. Nambissan, Three-dimensional finite element analysis of cracked thick plates in bending. *Int. J. Num. Meth. Engng* **19,** 293–303 (1983).
[3] H. Boduroglu and F. Erdogan, Internal and edge cracks in a plate of finite width under bending. *ASME J. appl. Mech.* **50,** 621–629 (1983).
[4] R. J. Hartranft and G. C. Sih, The use of eigenfunction expansions in the general solution of the three-dimensional crack problems. *J. Math. Mech.* **19,** 123–138 (1969).
[5] E. Hinton and J. S. Campbell, Local and global smoothing of discontinuous finite element functions using a least squares method. *Int. J. Num. Meth. Engng* **8,** 461–480 (1974).
[6] K. Keer and C. Sve, On the bending of cracked plates. *Int. J. Solids Struct.* **6,** 1545–1559 (1970).
[7] J. K. Knowles and N. M. Wang, On the bending of an elastic plate containing a crack. *J. Math. Phys.* **39,** 223–236 (1960).
[8] R. D. Mindlin, Influence of rotatory inertia and shear on flexural motions of isotropic elastic plates. *ASME J. appl. Mech.* **73,** 31 (1951).
[9] E. Reissner, On bending of elastic plates. *Q. appl. Math.* **V,** 55–68 (1947).
[10] J. R. Rice, A path-independent integral and the approximate analysis of strain concentration by notches and cracks. *ASME J. appl. Mech.* **35,** 379–386 (1968).
[11] V. L. Salerno and M. A. Goldberg, Effects of shear deformation on the bending of rectangular plates. *ASME J. appl. Mech.* **27,** 54–58 (1960).
[12] T. Watanabe, *et al.*, J-Integral analysis of plate and sheel structures with through-wall cracks using thick shell elements. *Engng Fracture Mech.* **19,** 1005–1012 (1984).
[13] Wen-Hwa Chen and Pei-Yen Chen, A hybrid-displacement finite element model for the bending analysis of thin cracked plates. *Int. J. Fracture* **24,** 83–106 (1984).
[14] G. Yagawa and T. Nishioka, Finite element analysis of stress intensity factors for plane extension and plate bending problems. *Int. J. Num. Meth. Engng* **14,** 727–740 (1979).
[15] T. Q. Ye and R. H. Gallagher, A singular finite element for analysis of plate bending problem in fracture mechanics. *Int. J. Fracture* **24,** 137–147 (1984).
[16] O. C. Zienkiewicz, *The Finite Element Method.* Third Edition, McGraw-Hill (1977).

(*Received* 12 *May* 1986).

APPENDIX

As mentioned in Section 4, appropriate use of the method of eigenfunction expansions in the Reissner's theory of plates, leads to the complete asymptotic behavior of relevant field quantities. The results are summarized for the leading terms in r in the sequel.

The components of the matrix γ referred to a polar coordinate system centered at the crack tip are given by

$$\begin{aligned}\psi_r = \frac{(1+\nu)}{E}\left(\frac{12}{h^3}\right)\Big\{&[B_0^{(1)}\cos\theta + B_0^{(2)}\sin\theta]\\ &+r^{1/2}\Big[-\frac{K_1}{2\sqrt{2}}\Big(\cos\frac{3\theta}{2}-\frac{5-3\nu}{1+\nu}\cos\frac{\theta}{2}\Big)+\frac{3K_2}{2\sqrt{2}}\Big(\sin\frac{3\theta}{2}-\frac{1}{3}\frac{5-3\nu}{1+\nu}\sin\frac{\theta}{2}\Big)\Big]\Big\}\\ &+rB_2^{(1)}\Big[\frac{1-\nu}{1+\nu}+\cos 2\theta\Big]\\ &+r^{3/2}\Big[\frac{8}{15}\frac{K_3}{(1+\nu)\sqrt{2}}\sin\frac{\theta}{2}\\ &+B_3^{(1)}\Big(\cos\frac{5\theta}{2}+\frac{3-5\nu}{1+\nu}\cos\frac{\theta}{2}\Big)+B_3^{(2)}\Big(\sin\frac{5\theta}{2}+\frac{1}{5}\frac{3-5\nu}{1+\nu}\sin\frac{\theta}{2}\Big)\Big]\Big\}\end{aligned}$$

$$\begin{aligned}\psi_\theta = \frac{(1+\nu)}{E}\left(\frac{12}{h^3}\right)\Big\{&[-B_0^{(1)}\sin\theta + B_0^{(2)}\cos\theta]\\ &+r^{1/2}\Big[-\frac{K_1}{2\sqrt{2}}\Big(-\sin\frac{3\theta}{2}+\frac{7-\nu}{1+\nu}\sin\frac{\theta}{2}\Big)+\frac{3K_2}{2\sqrt{2}}\Big(\cos\frac{3\theta}{2}-\frac{1}{3}\frac{7-\nu}{1+\nu}\cos\frac{\theta}{2}\Big)\Big]\\ &+r[C_2^{(2)}-B_2^{(1)}\sin 2\theta]\\ &+r^{3/2}\Big[\Big[8(1-\nu)-\frac{8}{15}\frac{9+\nu}{1+\nu}\Big]\frac{K_3}{(3-5\nu)\sqrt{2}}\cos\frac{\theta}{2}\\ &-B_3^{(1)}\Big(\sin\frac{5\theta}{2}-\frac{9+\nu}{1+\nu}\sin\frac{\theta}{2}\Big)+B_3^{(2)}\Big(\cos\frac{5\theta}{2}-\frac{1}{5}\frac{9+\nu}{1+\nu}\cos\frac{\theta}{2}\Big)\Big]\Big\}\end{aligned}$$

$$\begin{aligned}w = \frac{(1+\nu)}{E}\left(\frac{12}{h^3}\right)\Big\{&A_0^{(1)}+r^{1/2}\frac{2h^2}{5}\frac{K_3}{\sqrt{2}}\sin\frac{\theta}{2}\\ &+r[A_2^{(1)}\cos\theta - B_0^{(2)}\sin\theta]\\ &+r^{3/2}\Big[-\frac{1}{2}\frac{K_1}{\sqrt{2}}\Big(-\frac{2}{3}\frac{7+\nu}{1+\nu}\cos\frac{3\theta}{2}+2\frac{1-\nu}{1+\nu}\cos\frac{\theta}{2}\Big)\\ &+\frac{K_2}{\sqrt{2}}\frac{1-\nu}{1+\nu}\sin\frac{\theta}{2}+A_3^{(2)}\sin\frac{3\theta}{2}\Big]\Big\}\end{aligned}$$

where

$$A_0^{(1)},\ A_2^{(1)},\ A_3^{(2)},\ B_0^{(1)},\ B_0^{(2)},\ B_2^{(1)},\ B_3^{(1)},\ B_3^{(2)},\ C_2^{(2)}$$

are arbitrary constants. The quantities ψ_1 and ψ_2 can be calculated from the following transformation equations

$$\psi_1 = \psi_r\cos\theta - \psi_\theta\sin\theta$$

$$\psi_2 = \psi_r\sin\theta + \psi_\theta\cos\theta$$

The use of the above expressions for γ leads, through the constitutive relations, to the following components of $\mathbf{f}$ (where only the terms singular in r are taken into account)

$$M_{rr} = \frac{1}{4\sqrt{2r}}\Big\{-K_1\Big(\cos\frac{3\theta}{2}-5\cos\frac{\theta}{2}\Big)+3K_2\Big(\sin\frac{3\theta}{2}-\frac{5}{3}\sin\frac{\theta}{2}\Big)\Big\}$$

$$M_{\theta\theta} = \frac{1}{4\sqrt{2r}}\Big\{K_1\Big(\cos\frac{3\theta}{2}+3\cos\frac{\theta}{2}\Big)-3K_2\Big(\sin\frac{3\theta}{2}+\sin\frac{\theta}{2}\Big)\Big\}$$

$$M_{r\theta} = \frac{1}{4\sqrt{2r}}\Big\{K_1\Big(\sin\frac{3\theta}{2}+\sin\frac{\theta}{2}\Big)+3K_2\Big(\cos\frac{3\theta}{2}+\frac{1}{3}\cos\frac{\theta}{2}\Big)\Big\}$$

$$Q_r = \frac{K_3}{\sqrt{2r}}\sin\frac{\theta}{2}$$

$$Q_\theta = \frac{K_3}{\sqrt{2r}}\cos\frac{\theta}{2}.$$

The quantities M_{11}, M_{22}, M_{12}, Q_1, and Q_2 can be calculated from the following transformation formulae

$$M_{11} = M_{rr} \cos^2 \theta + M_{\theta\theta} \sin^2 \theta - 2M_{r\theta} \sin \theta \cos \theta$$

$$M_{22} = M_{rr} \sin^2 \theta + M_{\theta\theta} \cos^2 \theta + 2M_{r\theta} \sin \theta \cos \theta$$

$$M_{12} = (M_{rr} - M_{\theta\theta}) \sin \theta \cos \theta + M_{r\theta} (\cos^2 \theta - \sin^2 \theta)$$

$$Q_1 = Q_r \cos \theta - Q_\theta \sin \theta$$

$$Q_2 = Q_r \sin \theta + Q_\theta \cos \theta.$$